Natural frequency estimation by using torsional response, and applications for wind turbine drivetrain fault diagnosis

Natural frequency estimation by using torsional response, and applications for wind turbine drivetrain fault diagnosis

Farid K. Moghadam and Amir R. Nejad

Norwegian University of Science and Technology, Trondheim, Norway

E-mail: farid.k.moghadam@ntnu.no

Abstract. A method based on torsional vibration measurements for a system-level condition monitoring of the drivetrain system is developed in this paper. The latter is tested by using a $10MW$ wind turbine drivetrain simulation model, and experimentally validated by the drivetrain operational data obtained from a $1.75MW$ turbine. The method relies on the estimation of the drivetrain torsional natural frequencies by using the torsional responses residual function and subsequent monitoring of the variations in the eigenfrequencies and normal modes. In other words, an abnormal deviation from the reference values of these dynamic parameters can be translated into a meaningful interpretation on the propagation of a specific fault in the driveline. Local sensitivity analysis is employed to establish a relationship between different types of drivetrain faults and the system dynamic properties.

1 Introduction

Multi-megawatt offshore wind turbines are considered as a solution for the large-scale realization of renewable power generations. Offshore wind industry still suffers from longer downtime, high cost for repair and replacement of this system and higher risk of loss of turbine. The latter is due to the larger components and the difficulty to access the system in offshore environments, and a wider range of excitations due to the synergistic impacts of waves, currents and wind turbulences which call for innovative approaches to have a better understanding about the system dynamics and excitations. The focus of this research is proposing a system-level drivetrain condition monitoring (CM) solution by estimation and monitoring of the system dynamic properties. The latter is performed by developing a numerical model of the drivetrain as a dynamic system based on its measured torsional response and the subsequent estimation of torsional frequencies. The motivation is to reduce operational expenditure (OPEX) and subsequently levelized cost of energy (LCOE) to make offshore wind power competitive with land-based wind turbines.

Variations in the drivetrain can be monitored by tracking the changes in the modal parameters (resonance frequencies, damping ratios, and mode shapes) of the dominant modes of this system [1]. Operational modal analysis (OMA) approaches are proposed for characterization of the dynamic behavior (modal parameters) of wind turbine drivetrain in the recent literature by using the translational vibration measurements [1], which generally suffer from a high possibility that harmonics be misinterpreted as the eigenfrequencies [1, 2]. Drivetrain is a complex dynamical system with different sources of external excitations and components defect frequencies,and the

OMA techniques are still not matured enough for such a system. The latter has made OMA technique less-efficient for condition-based maintenance.

The possibility of estimating the drivetrain torsional natural frequencies by using the angular velocity residual function and the subsequent application for health monitoring of the drivetrain, blades and tower is discussed in this paper. Natural frequencies appear on torsional response (*e.g.* angular velocity) due to the impulsive behavior of wind which can act as a physical hammer which excites the system torsional frequencies. In addition, some wind and wave induced structural motions such as excited tower bending and blade in plane modes can act as torsional excitation sources and induce some torsional vibrations on the drivetrain torsional response. The latter makes the angular velocity measurements also applicable for health monitoring of tower and blades. The drivetrain system torsional response and the natural frequencies are proposed in the literature for detecting faults initiated by torsional sources. Patel *et al.* [3] proposes the use of angular displacement to support the lateral response to recognise the rubbing faults in the drivetrain, so that the excited torsional frequency and the amplitude of response in the natural frequency and the side bands are utilized to characterize the fault. Feng *et al.* [4] proposes the use of the measurements of torque instead of transverse vibration signals to diagnose planetary gearbox local/distributed faults, because they are free from the amplitude modulation effect caused by time variant vibration transfer paths, thus they have simpler spectral structure than transverse signals. Lebold *et al.* [5] suggests monitoring the characteristic changes in torsional natural frequencies, and claims that those changes are associated with the shaft crack propagation. Kia *et al.* [6] proposes the estimated electromagnetic torque of the electrical machine as a noninvasive torsional measurement in the drivetrain to monitor the torsional stress on the components including shaft, bearings, and gearbox, and the method is used to detect a gear failure. The electromagnetic torque estimation is commonly used in electrical drives to control the electrical machine, and implementation of the method does not need any additional sensor. Not only the drivetrain faults, but also rotor and tower excited modes can cause a torsional oscillation observable on the drivetrain torsional response [7, 8]. The amplitude of blade edgewise and tower bending natural frequencies can provide insights about resonances in these components. The monitoring of the variations of these components frequencies is also useful for some other purposes such as ice detection in blades, and health monitoring of blades (detect root cracks within turbine blades) and tower. The idea of using angular velocity measurements for the drivetrain fault detection is originally proposed by Nejad *et al.* [9]. The input data is provided from the encoders on the drivetrain used for the turbine control, and is normally in access in both the turbine and the farm levels. Therefore, any algorithm based on those measurements can simply be integrated in either turbine or farm control to support the online health monitoring of the drivetrain. Moghadam *et al.* [8] experimentally tests the potential of using the encoder measurements to detect different faults initiated by the different excitation sources, compared to a conventional method based on accelerometers.

In the proposed drivetrain condition monitoring approach of this paper, it is assumed that faults in the driveline (*e.g.* shaft cracks, unbalance and looseness) reveal themselves by variations in the system stiffness and moment of inertia. Therefore by monitoring the consequences of variations of drivetrain parameters (*i.e.* stiffness and moment of inertia matrices) in change of the drivetrain dynamic properties (*i.e.* natural frequencies, mode shapes and damping matrix), it is possible to monitor the progress of faults. For this purpose, a sensitivity analysis helps to realize what are the most influential parameters on the variability of the drivetrain dynamic properties. The main contributions of this work are:

(i) Estimation of the wind turbine drivetrain torsional natural frequencies by using the system torsional responses,

(ii) Estimation of the drivetrain damping in the torsional natural frequencies,

(iii) Proposing a method for driveline health monitoring without any additional sensor, based

on monitoring the variations in the estimated drivetrain dynamic properties.

2 Methodology

2.1 Torsional natural frequency estimation theory

The torsional response of equivalent one-degree-of-freedom rotational system in the non-dimensional form can be expressed by

$$\theta = \frac{\frac{\tau_0}{k_t}}{\sqrt{(1-(\frac{\omega}{\omega_n})^2)^2 + (2\zeta_t(\frac{\omega}{\omega_n}))^2}}, \tag{1}$$

where θ is the angular position and τ_0 is the amplitude of the excitation momentum. For this case, ω_n is the natural torsional frequency of the system. k_t is the torsional stiffness of the shaft, and ζ_t is the torsional damping ratio. An amplified frequency in the drivetrain torsional response can be due to a significant excitation amplitude or coincidence of excitation frequency with natural frequencies.

Natural frequencies appear on torsional responses *e.g.* angular velocity measurements due to impulsive behavior of wind which excites those frequencies. An initial velocity applied on a system as described by Thomson *et al.*[10] can play a role as an impact which is able to excite the system torsional frequencies. In the wind turbine, the ceaseless variations of wind results in continual variations in angular velocity which is physically similar to an initial velocity applied to the system. Though these variations in speed and subsequently torque are of a very low frequency and slow dynamics, but it introduces considerable energy in different frequencies including the characteristic frequencies of the system. Due to the existence of damping in a physical system, the measured natural frequencies from the torsional response are the damped frequencies. Our observations show that the angular velocity measurements can help to measure the drivetrain and the blade edgewise natural frequencies. By filtering the shafts revolution frequencies, components defect frequencies and excitations (very low frequency due to wind, low frequency due to wave tower shadow effect, and high frequency due to generator), the drivetrain torsional natural frequencies, and some torsional induced motions due to excited edgewise rotor blade and tower bending modes are acquired. Based on a primary knowledge on the torsional frequencies for each power range, it is possible to separate the observed natural frequencies for drivetrain, blades and tower. The variations in the natural frequencies and normal modes can be used as criteria for the severity of some sorts of faults in the drivetrain. To estimate the damped natural frequencies, angular velocity residual/error function is proposed. The input of this method is provided by two encoders located at the high- and low-speed shafts of drivetrain, and subsequently the residual function is constructed based on the subtraction of these two signals. Some drivetrains are only equipped with one angular velocity measurement on the shaft, so that the implementation of the method might require an additional moderate sampling frequency encoder to provide the sufficient inputs. The angular velocity residual function $e^{\omega}_{\mathrm{tot}}$ from the high-speed side is expressed by

$e^{\omega}_{tot} = \omega_{HS} - a_1 a_2 a_3 \omega_{LS}$, where ω_{HS} and ω_{LS} are the rotational speed in rad/s obtained from the high- and low-speed encoders, respectively. a_1, a_2 and a_3 are the inverse of gear ratios of the gearbox stages. The error function main feature is cancellation of the impacts of the excitations which are transferred to the drivetrain from the housing, from the resultant torsional response. Angular displacement and acceleration are the other torsional responses of the drivetrain system which could theoretically be used similar to angular velocity to obtain the system torsional parameters. For this purpose, similar to $e^{\omega}_{\mathrm{tot}}$, the angular displacement error function $e^{\theta}_{\mathrm{tot}}$ and the angular acceleration error function $e^{\alpha}_{\mathrm{tot}}$ are defined by

$e^{\theta}_{tot} = \theta_{HS} - a_1 a_2 a_3 \theta_{LS}, \quad \mathrm{e}^{\alpha}_{tot} = \alpha_{HS} - a_1 a_2 a_3 \alpha_{LS}.$

In particular, angular acceleration is the torsional response which has a direct relation with the applied load, and contains useful information on how the applied torque interacts with the

system. The frequency domain analytics Fourier transform and power spectral density (PSD) are used for analysis of the defined torsional response error functions. The Fourier series of $e^{\omega}_{\mathrm{tot}}$, $e^{\alpha}_{\mathrm{tot}}$ and $e^{\theta}_{\mathrm{tot}}$ are defined by

$$e^{\omega}_{tot}(\Omega) = \sum_{n=-\infty}^{\infty} C_n e^{ik_n\Omega},\ e^{\alpha}_{tot}(\Omega) = \sum_{n=-\infty}^{\infty} C_n(ik_n)e^{ik_n\Omega},\ e^{\theta}_{tot}(\Omega) = \sum_{n=-\infty}^{\infty} C_n(ik_n)^{-1}e^{ik_n\Omega}$$

Differentiation and integration are linear operations that are distributive over addition. As it can be seen, in $e^{\alpha}_{\mathrm{tot}}$ compared to $e^{\omega}_{\mathrm{tot}}$, the amplitude of the frequency components higher than 1 Hz is magnified with the gain k_{n}, and the frequencies lower than 1 Hz are weakened with the same proportion. In $e^{\theta}_{\mathrm{tot}}$ compared to $e^{\omega}_{\mathrm{tot}}$, the amplitude of the frequency components lower than 1 Hz is magnified with the gain k_{n}^{-1}, and the frequencies higher than 1 Hz are weakened with the same proportion.

The 1^{st} natural frequency of the drivetrain systems of the same technology decreases as the rated power increases. However, even for 10 MW wind turbine which is the highest commercially available and even for the high-speed technologies which have lower first natural frequencies, the first torsional frequency is higher than 1 Hz [11]. Therefore, the angular acceleration error functions theoretically outperforms the other two approaches in highlighting the torsional frequencies. The other benefit is weakening the frequencies lower than 1 Hz which appear in the drivetrain torsional response mostly due to wave and wind turbulence and does not contain any information on the natural frequencies. However, an additional derivation operation is required to attain acceleration from the velocity measurements which increases the computational cost of this method.

To evaluate the observability of natural frequencies on the torsional response error functions and the subsequent application for drivetrain condition monitoring, a simplified model of drivetrain is useful. The 1^{st} and 2^{nd} undamped natural frequencies (nonrigid modes) based on a simplified three-mass spring and three degrees of freedom (DOF) torsional model of a geared drivetrain is calculated by

$$\omega_n^1 = \sqrt{\frac{k_{LS}}{2J_{rot}} + \frac{k_{LS}+k_{HS}}{2J_{gear}} + \frac{k_{HS}}{2J_{gen}} - \sqrt{(\frac{-k_{LS}}{2J_{rot}} - \frac{k_{LS}-k_{HS}}{2J_{gear}} + \frac{k_{HS}}{2J_{gen}})^2 + \frac{k_{LS}k_{HS}}{J_{gear}^2}}}, \tag{2a}$$

$$\omega_n^2 = \sqrt{\frac{k_{LS}}{2J_{rot}} + \frac{k_{LS}+k_{HS}}{2J_{gear}} + \frac{k_{HS}}{2J_{gen}} + \sqrt{(\frac{-k_{LS}}{2J_{rot}} - \frac{k_{LS}-k_{HS}}{2J_{gear}} + \frac{k_{HS}}{2J_{gen}})^2 + \frac{k_{LS}k_{HS}}{J_{gear}^2}}}, \tag{2b}$$

where ω^1_{n} and ω^2_{n} are the 1^{st} and 2^{nd} natural frequencies, k_{LS} and k_{HS} are the torsional stiffness of low- and high-speed shafts, and J_{rot}, J_{gear} and J_{gen} are the moment of inertia of rotor, gearbox and generator, respectively.

2.1.1 Simulation based validation For the simulation studies, DTU 10 MW reference wind turbine is selected. In order to evaluate if the input torque is able to excite the drivetrain natural frequencies and subsequently to study the possibility of observing those frequencies in the different drivetrain torsional responses, an effective approach is involving decoupled simulation technique [12] and engaging frequency-domain data analytics. For this purpose, the rotor torque data of 10 MW turbine with a spar floating platform obtained from SIMA global simulation software is used, and the impacts on the drivetrain is studied using a decoupled analysis. The operating condition for this simulation is close to the rated operation with an average wind speed $U_w = 11\ m/s$, significant wave height $H_s = 3.5\ m$ and peak period $T_p = 7.5\ s$. The natural frequencies of the under consideration drivetrain is calculated by using a 3-DOF torsional model and eq. (2), and validated by Simpack multi-body simulation software. In this torsional model, rotor, gearbox and generator are modelled with equivalent moment of inertia, and the low-

and high-speed shafts are each modelled with a constant torsional stiffness. The generator and gearbox specifications are used from the optimized medium-speed 10 MW drivetrain system proposed in [11]. The parameters of this model are listed in Table 1. The natural frequencies of this model are 1.9 Hz and 73.9 Hz. The torsional responses of rotor and generator shafts are obtained from the Simpack simulated model to investigate possibility of observing the natural frequencies from the angular velocity, acceleration and displacement error functions.

Table 1: Model specification

Parameter	**Value**
Equivalent rotor moment of inertia J_{rot} $(kg.m^2)$	$800,000,000$
Equivalent gearbox moment of inertia J_{gear} $(kg.m^2)$	$1,239,300$
Equivalent generator moment of inertia J_{gen} $(kg.m^2)$	$15,716,775$
Equivalent low-speed shaft torsional stiffness K_{rot}^{gear} $(N.m/rad)$	$2,452,936,425$
Equivalent high-speed shaft torsional stiffness K_{gear}^{gen} $(N.m/rad)$	$245,293,642,500$

2.1.2 Experimental validation The operational data from Vestas V66-1.750MW turbine is used for the experimental study. To test the method, an additional encoder is installed on the low-speed shaft. In PSD of the angular velocity error function of the operational data, in addition to the natural frequencies, some other frequency components are also expected to be observed. However, by a prior knowledge about the defect frequencies and the other torsional excitation sources, and by subsequently filtering those frequencies, it is possible to distinguish the natural frequencies. The benefits with measuring the natural frequencies by this noninvasive method are the low implementation cost, and the possibility of obtaining the precise values of natural frequencies by including the system nonlinearities, and translational impacts on the rotation transferred through the bed-plate and torque arm.

2.2 Estimation of damping in the drivetrain

As discussed earlier, the natural frequencies measured by the approach proposed in Section 2.1 are the damped natural frequencies ω_d which have the relation $\omega_{\mathrm{d}}^i = \sqrt{(1-(\zeta^i)^2)}\omega_{\mathrm{n}}^i$ with the undamped frequency ω_{n}, with ζ^i the damping coefficient ($\zeta^i = c^i/c_{\mathrm{c}}^i$) for the i^{th} mode. c and c_{c} are actual and critical dampings. More precisely, the estimated natural frequencies are the extreme values of the response. The response extreme values from the simplified model in eq. (2.1), will occur at $\omega_{\mathrm{peak}}^i = \sqrt{(1-2(\zeta^i)^2)}\omega_{\mathrm{n}}^i$. ζ^i takes different values in different operating speeds. For two different operating speeds, for each frequency mode, damping in the system natural frequency of the two operations is related to the measured natural frequencies by eq. (3a)

$$\frac{\omega_{peak}^{i,t_1,\omega_1}}{\omega_{peak}^{i,t_2,\omega_2}} = \sqrt{\frac{1-(\zeta^{i,t_1,\omega_1})^2}{1-(\zeta^{i,t_2,\omega_2})^2}}, \quad (3a) \qquad \frac{\theta_{\omega_{peak}}^{i,t_1,\omega_1}}{\theta_{\omega_{peak}}^{i,t_2,\omega_2}} = \frac{\tau_0^{t_1}}{\tau_0^{t_2}}\frac{\zeta^{i,t_2,\omega_2}}{\zeta^{i,t_1,\omega_1}}\frac{\sqrt{1-(\zeta^{i,t_2,\omega_2})^2}}{\sqrt{1-(\zeta^{i,t_1,\omega_1})^2}}, \quad (3b) \qquad (3)$$

with $\omega_{\mathrm{peak}}^{i,t_1,\omega_1}$ the drivetrain eigenfrequency estimated during operation in the time period t_1 and the turbine speed ω_1. $\omega_{\mathrm{peak}}^{i,t_2,\omega_2}$ is the same parameter estimated during the time period t_2 and the speed ω_2. According to eq. (1), there is a relationship as shown in eq.(3b) between the amplitude of response and damping ratio at the measured natural frequencies for the two different operations. $\theta_{\omega_{\mathrm{peak}}}^{i,t_1,\omega_1}$ is the response amplitude in the i^{th} frequency mode in the operating point $\begin{bmatrix} t_1 \\ \omega_1 \end{bmatrix}$, and $\theta_{\omega_{\mathrm{peak}}}^{i,t_2,\omega_2}$ is the same parameter for the operating condition $\begin{bmatrix} t_2 \\ \omega_2 \end{bmatrix}$. To derive eq. (3$b$), it is assumed that the two operating points are close enough so that the stiffness and moment of inertia stay constant. As a result, the undamped natural frequency does not change. By using eqs (3a) and (3b), the absolute values of the damping coefficient of the system in the

natural frequency in different operating conditions can be estimated. The latter can be used to monitor damping in different operating speeds and helps to track the variations of damping over the system lifetime, which provides the input for retuning active dampers and helps to improve the system dynamic response. It is worth noting that the estimated damping by this methods also includes the effects of the rotor aerodynamic damping and active electric damping introduced by the generator control. Therefore, the resultant of damping of shafts, components, coupling and active dampers in the system natural frequencies can be observed which gives a good feedback for drivetrain design and also the operator for calibration of active damper parameters.

As it is shown in Section 2.3, the 1^{st} and 2^{nd} modes are affected to a great extent by the torsional stiffness of the low- and high-speed shafts, respectively. The damping of the first and second modes is also mostly dominated by the damping introduced by low- and high-speed shafts, respectively. Therefore, the estimated damping coefficients can be used to estimate the actual damping of the related shafts in the reduced order model of drivetrain.

The different damping behaviors in the system natural frequency compared to the harmonics in the torsional response is the criterion suggested for validating the natural frequencies estimated by the proposed method in Section 2.1. Based on eq. (1), damping is more significantly reducing the amplitude of response in the natural frequency compared to the harmonics, which helps to distinguish the natural frequency from the other harmonics. In other words, the ratio of amplitude of response at natural frequency in two different operating speeds is higher/lower (depended on if the speed drops or rises) than this ratio at harmonics.

2.3 Sensitivity analysis

A shaft crack results in reduction of the torsional stiffness of the shaft [13]. A change in the stiffness of the shafts also influences on the drivetrain system frequency modes. Therefore, by obtaining the mathematical relation between the stiffness of different shafts and the system natural frequencies, it is possible to monitor their conditions by monitoring variations in the natural frequencies. The other parameter which can influence on the drivetrain natural frequencies is the moment of inertia of the drivetrain components. Variations in the moment of inertia matrix represents the other category of faults in the driveline with the unbalance and looseness as the foremost. This category of faults are characterized by the increase of moment of inertia due to an additional force that is generated in those conditions and based on the parallel axis theorem. The mathematical relation between the drivetrain torsional natural frequencies and the moment of inertia of components can help to detect and localize these faults.

The variations in stiffness and moment of inertia can result in similar natural frequency variation patterns. Therefore, to distinguish between variations in the natural frequencies because of variations in the shafts' stiffness with those due to variations in moment of inertia matrix (source of fault), determining the correlation between the system parameters and the normalized mode shapes can provide a useful direction to find the source of fault. To check how the variations in stiffness and moment of inertia influence on the variability of system natural torsional frequencies and mode shapes, a sensitivity analysis is performed. There are two classes of sensitivity analysis methods, namely local and global sensitivity analysis. Morio *et al.*[14] has reported the same kind of results by using these two method for simple models. Local sensitivity determines how a small perturbation near an input parameter value influences the value of the output. In this Section, in order to find the parameters with the greatest impact on the drivetrain dynamic characteristics local sensitivity analysis is employed due to two main reasons. First, the motivation of this work is detecting faults in early stages for predictive maintenance purposes so that variations in the drivetrain system parameters happen with a slight change around the set point values. Second, local sensitivity analysis derives a closed form expression for the sensitivity value which makes the result more reliable and easier to implement. Local sensitivity is defined as the partial derivative of the output function with respect to the input parameters [15] as

$S_{i,j}^{Loc} = \frac{\delta y_i}{\delta x_j},\ y_i \in \{y_1, ..., y_p\}\ and\ x_j \in \{x_1, ..., x_q\}$, where y_{i} is the i^{th} output and x_{j} is the j^{th} input. To neutralize the impact of large/small inputs and small/large outputs, the local sensitivity can be normalized by the nominal values of inputs and outputs by

$S_{i,j}^{Norm} = \frac{x_j^{ref}}{y_i^{ref}} \frac{\delta y_i}{\delta x_j}$, with x_{j}^{ref} and y_{i}^{ref} as the nominal values of x_{j} and y_{i}. For the 3-DOF torsional model described in Section 2.1, the input and output vectors for sensitivity analysis are $x = \{k_{\mathrm{LS}},\ k_{\mathrm{HS}},\ J_{\mathrm{rot}},\ J_{\mathrm{gear}},\ J_{\mathrm{gen}}\}$ and $y = \{f_1^{tor},\ f_2^{tor}\}$. By applying normalized local sensitivity theory on eq. (2) we will have

$$S_{1,1}^{norm} = \frac{k_{LS}}{4} \frac{\frac{(\frac{1}{J_{gear}} + \frac{1}{J_{rot}})A - \frac{k_{HS}}{J_{gear}^2}}{\sqrt{A^2 + \frac{k_{LS}k_{HS}}{J_{gear}^2}}} + \frac{1}{J_{gear}} + \frac{1}{J_{rot}}}{-\sqrt{A^2 + \frac{k_{LS}k_{HS}}{J_{gear}^2}} + B},\quad S_{2,1}^{norm} = \frac{k_{LS}}{4} \frac{(\frac{1}{J_{gear}} - \frac{(\frac{1}{J_{gear}} + \frac{1}{J_{rot}})A - \frac{k_{HS}}{J_{gear}^2}}{\sqrt{A^2 + \frac{k_{LS}k_{HS}}{J_{gear}^2}}} + \frac{1}{J_{rot}})}{\sqrt{A^2 + \frac{k_{LS}k_{HS}}{J_{gear}^2}} + B}, \tag{4a}$$

$$S_{1,2}^{norm} = \frac{k_{HS}}{4} \frac{\frac{1}{J_{gen}} - \frac{(\frac{1}{J_{gear}} + \frac{1}{J_{rot}})A + \frac{k_{LS}}{J_{gear}^2}}{\sqrt{A^2 + \frac{k_{LS}k_{HS}}{J_{gear}^2}}} + \frac{1}{J_{gear}}}{-\sqrt{A^2 + \frac{k_{LS}k_{HS}}{J_{gear}^2}} + B},\quad S_{2,2}^{norm} = \frac{k_{HS}}{4} \frac{\frac{(\frac{1}{J_{gen}} + \frac{1}{J_{gear}})A + \frac{k_{LS}}{J_{gear}^2}}{\sqrt{A^2 + \frac{k_{LS}k_{HS}}{J_{gear}^2}}} + \frac{1}{J_{gen}} + \frac{1}{J_{gear}}}{\sqrt{A^2 + \frac{k_{LS}k_{HS}}{J_{gear}^2}} + B}, \tag{4b}$$

$$S_{1,3}^{norm} = -\frac{J_{rot}}{4} \frac{\frac{k_{LS}}{J_{rot}^2} + \frac{k_{LS}A}{J_{rot}^2\sqrt{A^2 + \frac{k_{LS}k_{HS}}{J_{gear}^2}}}}{-\sqrt{A^2 + \frac{k_{LS}k_{HS}}{J_{gear}^2}} + B},\quad S_{2,3}^{norm} = -\frac{J_{rot}}{4} \frac{\frac{k_{LS}}{J_{rot}^2} - \frac{k_{LS}A}{J_{rot}^2\sqrt{A^2 + \frac{k_{LS}k_{HS}}{J_{gear}^2}}})}{\sqrt{A^2 + \frac{k_{LS}k_{HS}}{J_{gear}^2}} + B}, \tag{4c}$$

$$S_{1,4}^{norm} = -\frac{J_{gear}}{4} \frac{\frac{k_{HS}+k_{LS}}{J_{gear}^2} - \frac{\frac{2k_{LS}k_{HS}}{J_{gear}^3} + \frac{(k_{HS}-k_{LS})A}{J_{gear}^2}}{\sqrt{A^2 + \frac{k_{LS}k_{HS}}{J_{gear}^2}}}}{-\sqrt{A^2 + \frac{k_{LS}k_{HS}}{J_{gear}^2}} + B},\quad S_{2,4}^{norm} = -\frac{J_{gear}}{4} \frac{\frac{\frac{2k_{LS}k_{HS}}{J_{gear}^3} + \frac{(k_{HS}-k_{LS})A}{J_{gear}^2}}{\sqrt{A^2 + \frac{k_{LS}k_{HS}}{J_{gear}^2}}} + \frac{k_{HS}+k_{LS}}{J_{gear}^2}}{\sqrt{A^2 + \frac{k_{LS}k_{HS}}{J_{gear}^2}} + B}, \tag{4d}$$

$$S_{1,5}^{norm} = -\frac{J_{gen}}{4} \frac{\frac{k_{HS}}{J_{gen}^2} - \frac{k_{HS}A}{J_{gen}^2\sqrt{A^2 + \frac{k_{LS}k_{HS}}{J_{gear}^2}}}}{-\sqrt{A^2 + \frac{k_{LS}k_{HS}}{J_{gear}^2}} + B},\quad S_{2,5}^{norm} = -\frac{J_{gen}}{4} \frac{\frac{k_{HS}}{J_{gen}^2} + \frac{k_{HS}A}{J_{gen}^2\sqrt{A^2 + \frac{k_{LS}k_{HS}}{J_{gear}^2}}}}{\sqrt{A^2 + \frac{k_{LS}k_{HS}}{J_{gear}^2}} + B}, \tag{4e}$$

where $A = \frac{k_{HS}}{2J_{gen}} - \frac{k_{LS}}{2J_{rot}} + \frac{k_{HS}-k_{LS}}{2J_{gear}}$ and $B = \frac{k_{HS}}{2J_{gen}} + \frac{k_{LS}}{2J_{rot}} + \frac{k_{HS}+k_{LS}}{2J_{gear}}$.

A schematic figure representing the proposed driveline condition monitoring method is illustrated in Fig. 1. $EN1$ and $EN2$ in this figure are the angular velocity measurement sensors placed on the low- and high-speed shafts, respectively. The algorithm which summarizes the proposed approach is depicted in Fig. 2. $\varphi^{1,m}$ and $\varphi^{2,m}$ are the normal modes related to the 1^{st} and 2^{nd} natural frequencies, respectively. m varies from 1 up to the degree of the model. τ and $\tau_{\varphi \mathrm{m}}$ are the low-limit threshold natural frequency and normal mode for normal operations. It is worth noting that the natural frequencies estimated and subsequently used in the condition monitoring algorithm are the damped natural frequencies which are directly estimated from the operational measurements of system torsional response. In order to eliminate the influence of different damping values as a result of different turbine operational speeds, the estimated natural frequencies and the associated thresholds are engaged in the proposed algorithm based on the operational speed.

3 Results

3.1 Simulation results

The PSD spectrum of angular velocity error function obtained from 10 MW drivetrain model in Simpack and its capability in highlighting the torsional natural frequencies is shown in Fig.

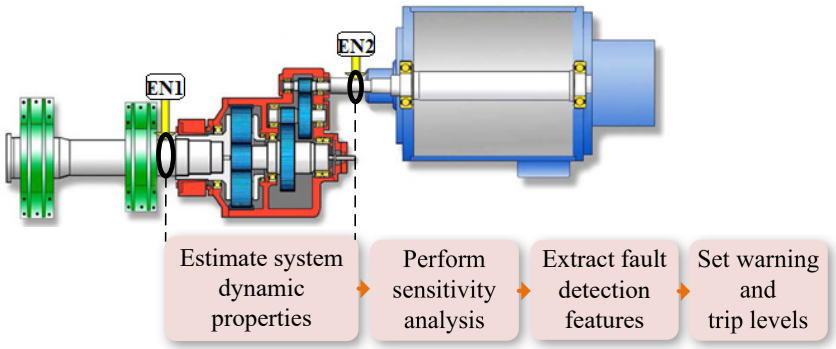

Figure 1: Schematic of the proposed condition monitoring method.

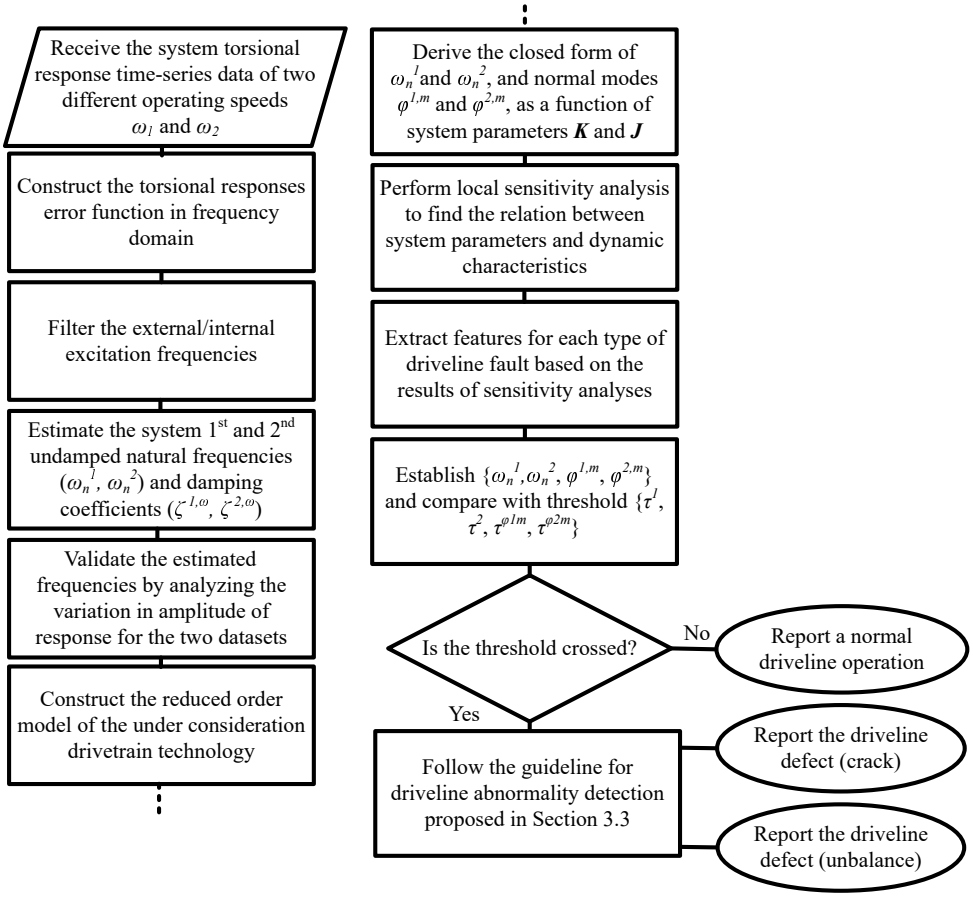

Figure 2: Flowchart of the proposed algorithm for driveline condition monitoring.

3. In this figure, the performance of angular velocity error function in extracting the 1^{st} and 2^{nd} torsional natural frequencies of the drivetrain is compared with angular displacement and angular acceleration error functions. As it can be seen, acceleration error function outperforms in revealing the higher frequency modes (the 2^{nd} mode). The higher modes have usually a lower impact on the response, which impedes disclosure of those frequencies. The PSD spectrum of input torque obtained from the global simulation and applied on the Simpack drivetrain model is shown in Fig. 3a. This input contains the majority of frequency components and can excite the drivetrain natural frequencies. In this simulation study, the model is undamped. Therefore, the estimated frequencies are the undamped frequencies. As discussed in Section 2.2, for a damped system, the estimated frequencies are the peak frequencies which can be translated to

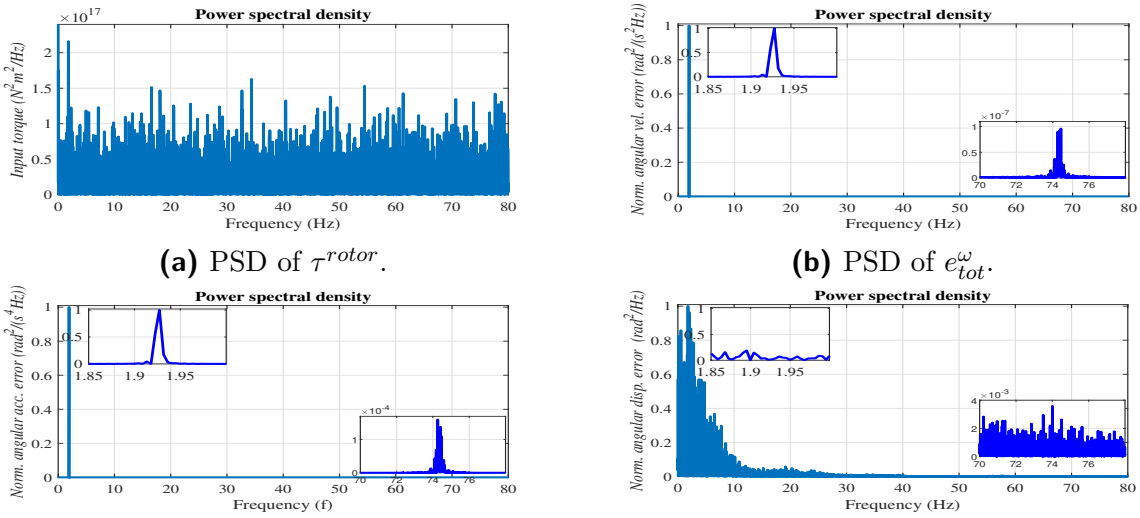

(a) PSD of τ^{rotor}. **(b)** PSD of e^{ω}_{tot}.

(c) PSD of e^{α}_{tot}. **(d)** PSD of e^{θ}_{tot}.

Figure 3: Simulation results based on 10 MW floating wind turbine model.

the undamped natural frequencies by using the estimated damping coefficients from the theory elaborated in the same Section. ω_{n} can also be approximated with ω_{peak} if $\zeta << 1$ which may not be an unrealistic assumption for multi-megawatt wind turbine drivetrain systems.

3.2 Experimental results

The PSD spectrum of angular velocity error function of the Vestas drivetrain operational data for a rated operation is shown in Fig. 4, which shows the observability of both the drivetrain and blade natural frequencies. The results are validated by comparing with the 1^{st} drivetrain and 1^{st} blade edgewise natural frequencies of another turbine with the same drivetrain technology and a similar power range reported in [16]. The performance of angular velocity error function is compared with angular displacement and acceleration error functions. As it can be seen, angular acceleration shows a slightly higher performance in amplification and extraction of characteristic frequencies of higher values.

A comparison between the angular velocity error function PSD in two different operating speeds is shown in Fig. 4d. As it can be seen, the higher damping coefficient in lower speeds results in a lower damped natural frequency as discussed in Section 2.2. Furthermore, at the drivetrain natural frequency, the amplitude reacts more significantly to the variation in damping. In other words, the amplitude of response at the natural frequency reduces more compared with other harmonics, for a lower rotor speed which corresponds to a higher damping.

3.3 Sensitivity analysis results

The results of the normalized local sensitivity analyses with natural frequencies (f_1^{tor}, f_2^{tor}) and normal modes (ϕ_1, ϕ_2) as the outputs and shaft stiffnesses ($K_{\mathrm{LS}}, K_{\mathrm{HS}}$) as the inputs are shown in Table 2. The reported numbers show the normalized sensitivity values and also the variations of outputs (in %) for the input parameters changed by $\pm 5\%$ of their rated values. As it can be seen, there is a direct relationship between the 1^{st} frequency and K_{LS}, and the 2^{nd} frequency and K_{HS}. Therefore, variations in the natural frequencies can be translated into the variations in the shaft stiffness and subsequently the defects in the drivetrain shafts. The influence of the shafts defect (stiffness variation) on amplitude of oscillation due to the 1^{st} mode is negligible. However, the stiffness variation results in variations in the amplitude of oscillation in rotor due to the 2^{nd} mode.

The results of the sensitivity analyses with natural frequencies and normal modes as the outputs

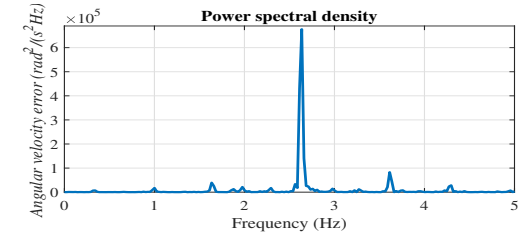

(a) PSD of e^{ω}_{tot}.

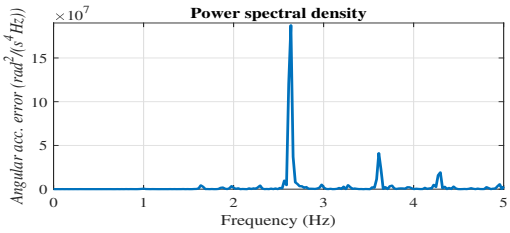

(b) PSD of e^{α}_{tot}.

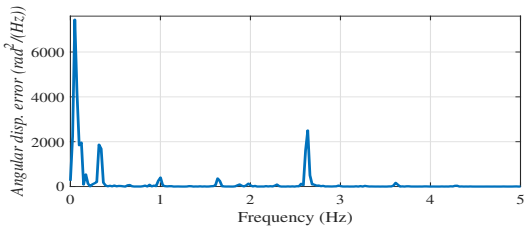

(c) PSD of e^{θ}_{tot}.

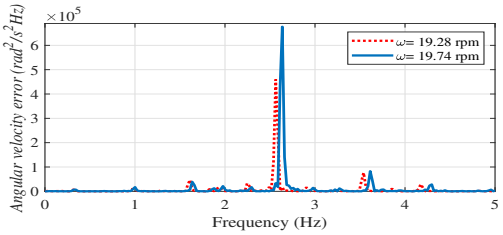

(d) velocity (different operations).

Figure 4: Experimental results based on 1.75 MW Vestas turbine operational data.

Table 2: Sensitivity of natural frequencies, amplitude of oscillation due to the 1^{st} mode, and amplitude of oscillation due to the 2^{nd} mode to torsional stiffness.

Sensitivity \ Variable	$K_{LS}(\pm5\%)$	$K_{HS}(\pm5\%)$	K_{LS} *and* K_{HS} $(\pm5\%)$
f_1^{tor}	$0.50(\pm2.48\%)$	$0.00(\pm0.02\%)$	$0.50(\pm2.50\%)$
f_2^{tor}	$0.00(\pm0.02\%)$	$0.50(\pm2.48\%)$	$0.50(\pm2.50\%)$
ϕ_1^{rot}	$0.00(\pm0.02\%)$	$0.00(\mp0.02\%)$	$0.00(0.00\%)$
ϕ_1^{gear}	$0.00(\mp0.02\%)$	$0.00(\pm0.02\%)$	$0.00(0.00\%)$
ϕ_1^{gen}	$0.00(\pm0.02\%)$	$0.00(\mp0.02\%)$	$0.00(0.00\%)$
ϕ_2^{rot}	$0.99(\pm4.96\%)$	$-0.99(\mp4.97\%)$	$0.00(0.00\%)$
ϕ_2^{gear}	$0.00(0.00\%)$	$0.00(0.00\%)$	$0.00(0.00\%)$
ϕ_2^{gen}	$-0.01(\mp0.05\%)$	$0.01(\pm0.05\%)$	$0.00(0.00\%)$

and moment of inertia $(J_{\text{rot}}, J_{\text{gear}}, J_{\text{gen}})$ as the inputs are shown in Table 3. As it can be seen, there is an inverse relationship between the 1^{st} frequency and J_{gen}, and the 2^{nd} frequency and J_{gear}, so that the reduction of natural frequencies can be due to a rise in the moment of inertia. To distinguish between the drop in natural frequencies due to variation in stiffness and moment of inertia, the results should be interpreted together with monitoring the variations of normal modes. The simultaneous drop of the 1^{st} frequency and the amplitude of oscillation at rotor due to the 2^{nd} mode represents a problem in low-speed shaft. The drop of the 2^{nd} frequency and the simultaneous rise in amplitude of oscillation at rotor due to the 2^{nd} mode discloses the problems in high-speed shaft. The drop of the 1^{st} frequency, the simultaneous rise in amplitude of oscillation at rotor due to the 1^{st} mode and drop in amplitude of oscillation at generator due to the 2^{nd} mode reveal unbalances in generator side. The drop of the 2^{nd} frequency and a simultaneous rise in amplitude of oscillation at both rotor and generator due to the 2^{nd} mode can be used as the criteria to detect an unbalance in gearbox. However, unbalance in rotor represents it self mainly by variations in normal modes with minor influence on the natural frequencies,so that a simultaneous drop in amplitude of oscillation at rotor due to 1^{st} and 2^{nd} modes are indicators of rotor unbalance.

4 Conclusions

The potentials of using drivetrain torsional responses for estimation of the drivetrain torsional natural frequencies and heath monitoring of the driveline was discussed, and evaluated by both experimental and simulation studies. Local sensitivity analysis was engaged to find the

Table 3: Sensitivity of natural frequencies, amplitude of oscillation due to the 1^{st} mode, and amplitude of oscillation due to the 2^{nd} mode to moment of inertia.

Variable / Sensitivity	$J_{rot}(\pm5\%)$	$J_{gear}(\pm5\%)$	$J_{gen}(\pm5\%)$	$J_{rot}(\pm5\%)$ $J_{gear}(\pm5\%)$	$J_{gear}(\pm5\%)$ $J_{gen}(\pm5\%)$	$J_{rot}(\pm5\%)$ $J_{gen}(\pm5\%)$	$J_{rot}(\pm5\%)$ $J_{gear}(\pm5\%)$ $J_{gen}(\pm5\%)$
f_1^{tor}	$-0.01(\mp0.05\%)$	$-0.03(\mp0.17\%)$	$-0.45(\mp2.25\%)$	$-0.40(\mp0.22\%)$	$-0.49(\mp2.44\%)$	$-0.46(\mp2.32\%)$	$-0.50(\mp2.50\%)$
f_2^{tor}	$0.00(0.00\%)$	$-0.45(\mp2.25\%)$	$-0.04(\mp0.18\%)$	$-0.45(\mp2.25\%)$	$-0.49(\mp2.44\%)$	$-0.04(\mp0.18\%)$	$-0.49(\mp2.44\%)$
ϕ_1^{rot}	$-1.00(\mp5.01\%)$	$0.07(\pm0.35\%)$	$0.93(\pm4.63\%)$	$-0.93(\mp4.66\%)$	$1.00(\pm4.98\%)$	$-0.07(\mp0.37\%)$	$0.00(\mp0.02\%)$
ϕ_1^{gear}	$0.00(0.00\%)$	$0.00(0.00\%)$	$0.00(0.00\%)$	$0.00(0.00\%)$	$0.00(0.00\%)$	$0.00(0.00\%)$	$0.00(0.00\%)$
ϕ_1^{gen}	$0.00(0.00\%)$	$0.00(0.00\%)$	$0.00(0.00\%)$	$0.00(0.00\%)$	$0.00(0.00\%)$	$0.00(0.00\%)$	$0.00(0.00\%)$
ϕ_2^{rot}	$-1.00(\mp5.01\%)$	$0.89(\pm4.47\%)$	$0.08(\pm0.39\%)$	$-0.10(\mp0.52\%)$	$0.97(\pm4.85\%)$	$-0.92(\mp4.62\%)$	$-0.03(\mp0.14\%)$
ϕ_2^{gear}	$0.00(0.00\%)$	$-0.01(\mp0.03\%)$	$0.01(\pm0.03\%)$	$-0.01(\mp0.03\%)$	$0.00(0.00\%)$	$0.01(\pm0.03\%)$	$0.00(0.00\%)$
ϕ_2^{gen}	$0.00(0.00\%)$	$0.96(\pm4.82\%)$	$-1.00(\mp4.98\%)$	$0.96(\pm4.82\%)$	$-0.03(\mp0.15\%)$	$-1.00(\mp4.98\%)$	$-0.03(\mp0.15\%)$

mathematical relation between the variations in dynamic properties of the system and variations in drivetrain parameters. In order to detect and localize the driveline faults, one should look into the variations in the system natural frequencies and the amplitude of oscillation due to the frequency modes. Future work will be focused on applying the proposed approach on more detailed models of the drivetrain to cover more diversity of faults in the driveline, and using the technique for prognosis of the driveline faults in various drivetrain technologies.

References

[1] El-Kafafy, M., Gioia, N., Guillaume, P. and Helsen, J., 2019. Long-term automatic tracking of the modal parameters of an offshore wind turbine drivetrain system in standstill condition. *In Rotating Machinery, Vibro-Acoustics & Laser Vibrometry*, Vol. 7 (pp. 91-99).

[2] El-Kafafy, M., Colanero, L., Gioia, N., Devriendt, C., Guillaume, P. and Helsen, J., 2017. Modal parameters estimation of an offshore wind turbine using measured acceleration signals from the drivetrain. *In Struc. Health Monitoring& Damage Detection*, 7, pp.41-48.

[3] Patel, T.H. and Darpe, A.K., 2009. Coupled bending-torsional vibration analysis of rotor with rub and crack. *Journal of Sound and Vibration*, 326(3-5), pp.740-752.

[4] Feng, Z. and Zuo, M.J., 2013. Fault diagnosis of planetary gearboxes via torsional vibration signal analysis. *Mechanical Systems and Signal Processing*, 36(2), pp.401-421.

[5] Lebold, M.S., Maynard, K., Reichard, K., Trethewey, M., Bieryla, D., Lissenden, C. and Dobbins, D., 2004, March. Using torsional vibration analysis as a synergistic method for crack detection in rotating equipment. *IEEE Aerospace Conf. Proc.*, Vol. 6, pp. 3517-3527.

[6] Kia, S.H., Henao, H. and Capolino, G.A., 2009. Torsional vibration assessment using induction machine electromagnetic torque estimation. *IEEE Transactions on Industrial Electronics*, 57(1), pp.209-219.

[7] Lu, B., Li, Y., Wu, X. and Yang, Z., 2009, June. A review of recent advances in wind turbine condition monitoring and fault diagnosis. *In 2009 IEEE Power Electronics and Machines in Wind Applications*, pp. 1-7.

[8] Moghadam, F.K., and Nejad, A.R., 2019. Experimental validation of angular velocity measurements for wind turbines drivetrain condition monitoring. *Accepted by Proceedings of* 2^{nd} *International Offshore Wind Technical Conference (IOWTC) 2019.*

[9] Nejad, A.R., Odgaard, P.F. and Moan, T., 2018. Conceptual study of a gearbox fault detection method applied on a 5-MW spar-type floating wind turbine. *Wind Energy*, 21(11), pp.1064-1075.

[10] Thomson, W., 2018. Theory of vibration with applications. CrC Press.

[11] Moghadam, F.K., and Nejad, A.R., 2019. Evaluation of PMSG-based drivetrain

technologies for 10 MW floating offshore wind turbines: pros and cons in a life-cycle perspective. *Accepted by Wind Energy.*

[12] Nejad, A.R., Bachynski, E.E. and Moan, T., 2019. Effect of axial acceleration on drivetrain responses in a spar-type floating wind turbine. *Journal of Offshore Mechanics and Arctic Engineering*, 141(3).

[13] Lissenden, C.J., Tissot, S.P., Trethewey, M.W. and Maynard, K.P., 2007. Torsion response of a cracked stainless steel shaft. *Fatigue and fracture of engineering materials and structures*, 30(8), pp.734-747.

[14] Morio, J., 2011. Global and local sensitivity analysis methods for a physical system. *European Journal of Physics*. 32. 1577.

[15] Saltelli, A., Tarantola, S. and Chan, K.S., 1999. A quantitative model-independent method for global sensitivity analysis of model output. *Technometrics*, 41(1), pp.39-56.

[16] Licari, J., Ugalde-Loo, C.E., Ekanayake, J.B. and Jenkins, N., 2012. Damping of torsional vibrations in a variable-speed wind turbine. *IEEE Transactions on Energy Conversion*, 28(1), pp.172-180.